CellPress

Neuron
Article

Separate Microcircuit Modules of Distinct V2a Interneurons and Motoneurons Control the Speed of Locomotion

Konstantinos Ampatzis,[1,2] Jianren Song,[1,2] Jessica Ausborn,[1] and Abdeljabbar El Manira[1,*]
[1]Department of Neuroscience, Karolinska Institute, 171 77 Stockholm, Sweden
[2]Co-first Authors
*Correspondence: Abdel.ElManira@ki.se
http://dx.doi.org/10.1016/j.neuron.2014.07.018

SUMMARY

Spinal circuits generate locomotion with variable speed as circumstances demand. These circuits have been assumed to convey equal and uniform excitation to all motoneurons whose input resistance dictates their activation sequence. However, the precise connectivity pattern between excitatory premotor circuits and the different motoneuron types has remained unclear. Here, we generate a connectivity map in adult zebrafish between the V2a excitatory interneurons and slow, intermediate, and fast motoneurons. We show that the locomotor network does not consist of a uniform circuit as previously assumed. Instead, it can be deconstructed into three separate microcircuit modules with distinct V2a interneuron subclasses driving slow, intermediate, or fast motoneurons. This modular design enables the increase of locomotor speed by sequentially adding microcircuit layers from slow to intermediate and fast. Thus, this principle of organization of vertebrate spinal circuits represents an intrinsic mechanism to increase the locomotor speed by incrementally engaging different motor units.

INTRODUCTION

Spinal circuits generate coordinated locomotion (Arber, 2012; Büschges et al., 2011; Grillner and Jessell, 2009; Kiehn, 2006). They are endowed with the capacity to increase the locomotor speed by sequentially recruiting different types of motor units (Ampatzis et al., 2013; Burke, 2011; Gabriel et al., 2011; Henneman and Mendell, 1981; Hoffer et al., 1987; Liddell and Sherrington, 1925; McLean et al., 2007, 2008; Zhang et al., 2011). The "size principle" assumes that all motoneuron types from slow to fast receive a homogenous and uniformly distributed excitatory drive. The input resistance has been considered the crucial property dictating the sequence of recruitment of motoneurons (Cope and Pinter, 1995; Goulding, 2009; Grillner and Jessell, 2009; Gustafsson and Pinter, 1984; Henneman, 1957; Henneman and Mendell, 1981; Kiehn, 2006; Roberts et al., 2010). However, it is unclear if the locomotor premotor network forms a uniform unit that conveys equal excitatory inputs to all motoneurons or whether the different motoneurons are embedded in separate microcircuits and are preferentially connected to distinct groups of excitatory premotor interneurons. A distinction between these two alternatives requires a precise mapping of connectivity between the excitatory interneurons and the different types of motoneurons.

The unfavorable architecture of muscles and motor pools organization in mammals with spatially intermingled slow, intermediate, and fast units makes it difficult to define the connectivity rules within the spinal circuits and their relationship to speed control (Burke, 2011; Dasen and Jessell, 2009; Henneman and Mendell, 1981; Romanes, 1964). In the adult zebrafish, the muscle types and motoneurons are well separated (Lewis and Eisen, 2003; van Raamsdonk et al., 1982). We previously showed that during swimming there is a gradual activation of motoneurons with increased speed that relates to the properties of the muscles they innervate (Ampatzis et al., 2013). An important source of excitation within the spinal circuits of zebrafish are the V2a interneurons, which represent a class of glutamatergic interneurons with ipsilateral axonal projections (Bernhardt et al., 1990; Hale et al., 2001). This interneuron class is defined by the expression of the transcription factor Chx10 (Kimura et al., 2006, 2013). Selective activation of the V2a interneurons using optogenetic tools is sufficient for the generation of a coordinated locomotor pattern (Eklöf-Ljunggren et al., 2012; Ljunggren et al., 2014). It is still unclear if the V2a interneurons are segregated into functionally distinct subclasses that are selectively connected to the different motoneuron types. In addition, it is crucial to uncover the functional connectivity map between subclasses of V2a interneurons and motoneurons within the spinal circuits to be able to account for the sequential activation of motor units at different speeds of locomotion.

We investigated the functional organization of V2a interneurons and their precise pattern of connectivity with motoneurons. Our results show that the V2a interneurons are subdivided into three functional subclasses recruited at slow, intermediate, and fast swimming frequencies. In addition, we show that the locomotor network does not consist of a uniform circuit that conveys equal excitation to slow, intermediate, and fast motoneuron pools. This invalidates the "size principle" assumption of equal excitation to all motoneurons. Instead, we reveal that the adult zebrafish spinal locomotor network is composed of

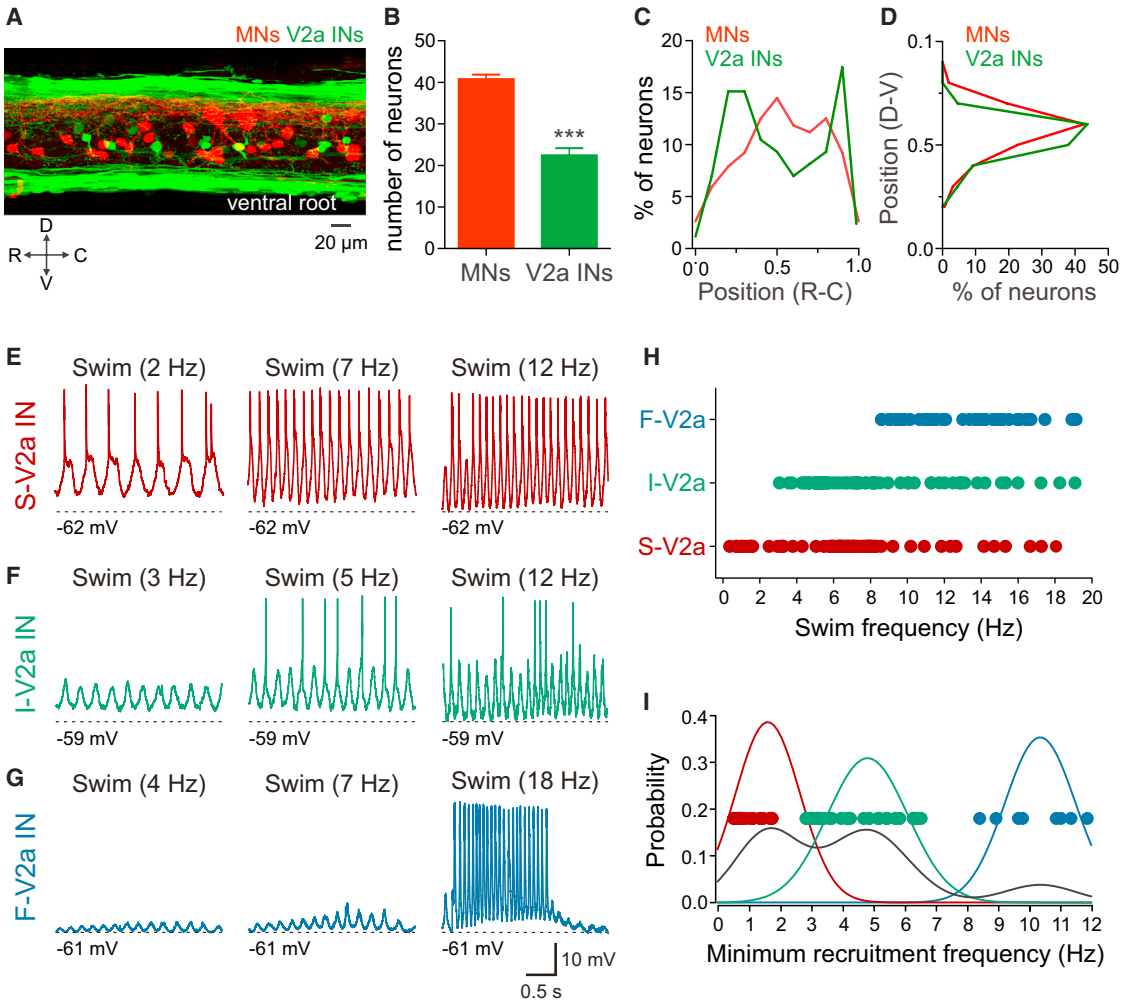

Figure 1. Organization and Activation Pattern of V2a Interneurons

(A) A side view of a hemisegment of the adult zebrafish spinal cord showing the distribution of V2a interneurons expressing GFP (green) and motoneurons retrogradely labeled with rhodamine dextran (red).

(B) The number of motoneurons per hemisegment was significantly higher than that of V2a interneurons. Each bar represents the mean ± SEM from six different preparations.

(C) Motoneurons and V2a interneurons showed an overlapping distribution along the rostrocaudal (R-C) axis of a spinal cord segment.

(D) Motoneurons and V2a interneurons displayed an overlapping distribution along the dorsoventral (D-V) axis of the spinal cord.

(E) Recordings of a slow V2a interneurons (S-V2a IN) showing that it was recruited at all swimming frequencies from slow to fast.

(F) An intermediate V2a interneurons (I-V2a IN) that became recruited at intermediate swimming frequencies and remained active at higher frequencies.

(G) A fast V2a interneuron (F-V2a IN) that received subthreshold synaptic inputs at slow and intermediate swimming frequencies and was recruited only at high frequencies.

(H) The different V2a interneuron subclasses were recruited in a stepwise manner at a specific frequency threshold during swimming.

(I) Graph showing the distribution of the minimum recruitment frequencies of the different subclasses of V2a interneurons (black trace). A Gaussian mixture model analysis revealed three normal distributions corresponding to slow (red), intermediate (green), and fast (blue) V2a interneuron subclasses. The filled circles indicate the minimum recruitment frequencies of individual V2a interneurons belonging to slow (red), intermediate (green), and fast (blue) subclasses.

three separate microcircuit modules, encompassing distinct V2a interneuron subclasses that selectively make excitatory synaptic connections with slow, intermediate, and fast motoneuron pools, respectively. This selective modular design allows for the increase of locomotor speed by sequentially engaging successive microcircuit layers (V2a interneurons-motoneurons) from slow to intermediate and fast. Such a multiple microcircuit organization may represent a general feature of vertebrate locomotor networks that endows them with an intrinsic mechanism to increase speed and force of movements.

RESULTS

Organization and Activation Pattern of V2a Interneurons

We first examined the anatomical organization of V2a interneurons and compared it to that of motoneurons in an individual

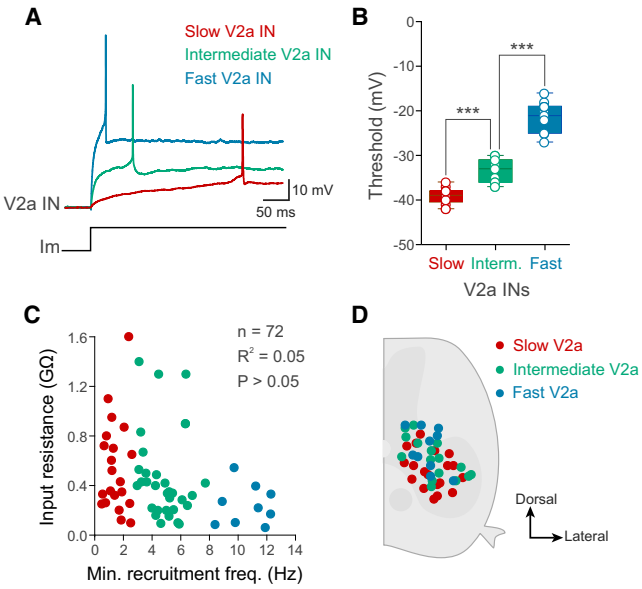

Figure 2. Properties of V2a Interneurons and Their Relationship to Their Pattern of Recruitment

(A) The different subclasses of V2a interneurons displayed a different action potential threshold as determined by current injection in individual interneurons.

(B) There was a significant difference in the action potential threshold between slow (red), intermediate (green), and fast (blue) V2a interneurons.

(C) There was no correlation between the order of recruitment of the different V2a interneurons and their input resistance.

(D) Lack of topographic organization of the different subclasses of V2a interneurons. Slow (red), intermediate (green), and fast (blue) V2a interneurons were intermingled in the spinal column.

hemisegment (segment 11) located rostral to the dorsal fin of the adult zebrafish. For this we retrogradely labeled motoneurons with rhodamine dextran in transgenic animals expressing GFP in V2a interneurons. There were significantly more motoneurons (41.0 ± 1.0; mean ± SEM; n = 6 preparations) than V2a interneurons (22.5 ± 1.6) per hemisegment (Figures 1A and 1B). Both motoneurons and V2a interneurons showed an overlapping distribution along the rostrocaudal and dorsoventral axes of a given spinal cord segment (Figures 1A, 1C, and 1D). Second, we examined how the recruitment pattern of V2a interneurons maps onto that of the slow, intermediate, and fast motoneuron pools during swimming (Ampatzis et al., 2013). For this we made whole-cell patch-clamp recordings from individual V2a interneurons (n = 72) using a transgenic zebrafish line with GFP expression driven by the Chx10 promoter (Kimura et al., 2006) (Figure 1A). Locomotor activity was induced by stimulation of descending axons from the brainstem (Kyriakatos et al., 2011), and the activity of the individual interneurons was assessed at different locomotor burst frequencies. Similar to motoneurons, the V2a interneurons could be subdivided into three subclasses (slow, intermediate, and fast) based on their threshold frequency at which they were recruited (Figures 1E–1G). V2a interneurons of the slow subclass were always activated at the onset of locomotor activity and remained active at higher frequencies (Figures 1E and 1H). The intermediate subclass was activated at frequencies exceeding 3 Hz (Figures 1F and 1H). Finally, the fast subclass became active only when the locomotor frequencies exceeded 8 Hz (Figures 1G and 1H). The subdivision of V2a interneurons into three subclasses was further supported by analyzing the distribution of their minimum recruitment frequencies (Figure 1I). Indeed, three main clusters of V2a interneurons emerge using a Gaussian mixture model analysis of their minimum recruitment frequencies (Figure 1I). The minimum recruitment frequency of slow, intermediate, and fast V2a interneuron subclasses were clearly separated by gaps of 1 to 2 Hz (Figure 1I).

The three V2a interneuron subclasses displayed a significant difference in their action potential thresholds, which were graded in a manner reflecting their order of activation during swimming (Figures 2A and 2B). The threshold was lowest in the slow V2a interneuron (−39.2 ± 0.8 mV; n = 13), highest in the fast subclass (−21.4 ± 0.9 mV; n = 14), and that of the intermediate V2a interneurons ranging in between (−33.5 ± 0.8 mV; n = 11). However, there was no correlation between the input resistance of the different V2a interneurons and their minimum recruitment frequency (Figure 2C). Finally, the soma of the different V2a interneurons subclasses were not organized topographically but were intermingled in the spinal column (Figure 2D).

These results show that the V2a interneurons form a functionally heterogeneous population organized into three subclasses that are added in a stepwise manner during swimming with increased frequency. Their order of recruitment neither follows topography nor is dictated by the input resistance.

Selective Pattern of Connectivity between Subclasses of V2a Interneurons and Motoneurons

There is a clear correspondence between the organization and recruitment pattern of V2a interneurons and motoneurons. Both are organized in three distinct subclasses that are sequentially engaged in an orderly manner with increased speeds of locomotion from slow to intermediate and fast. To test if this correspondence reflects a selective connectivity pattern, we performed a detailed connectivity map using dual whole-cell patch-clamp recordings from V2a interneurons and motoneurons (Figure 3A). First, we showed that single action potentials in V2a interneurons induced monosynaptic glutamatergic excitatory postsynaptic potentials (EPSPs) in motoneurons (Figures 3B and 3C). These monosynaptic connections showed variable strength with strong, weak, or no connections. Strong connections were characterized by relatively large EPSPs (amplitude > 0.1 mV) that were elicited both by single and trains of action potentials in V2a interneurons (Figure 3D). Weak connections were characterized by relatively small EPSPs (amplitude < 0.06 mV) elicited by single action potentials that summated during repetitive stimulation of the presynaptic V2a interneuron (Figure 3E). In pairs with no connections, EPSPs were induced in motoneurons neither by single nor by trains of action potentials in V2a interneurons (Figure 3F).

Second, we tested if the difference in the strength of the synaptic connections relates to a selective pattern of connectivity between slow, intermediate, or fast V2a interneurons and motoneurons by performing a detailed mapping of their synaptic connections (n = 113 pairs; Figure 4). It became apparent

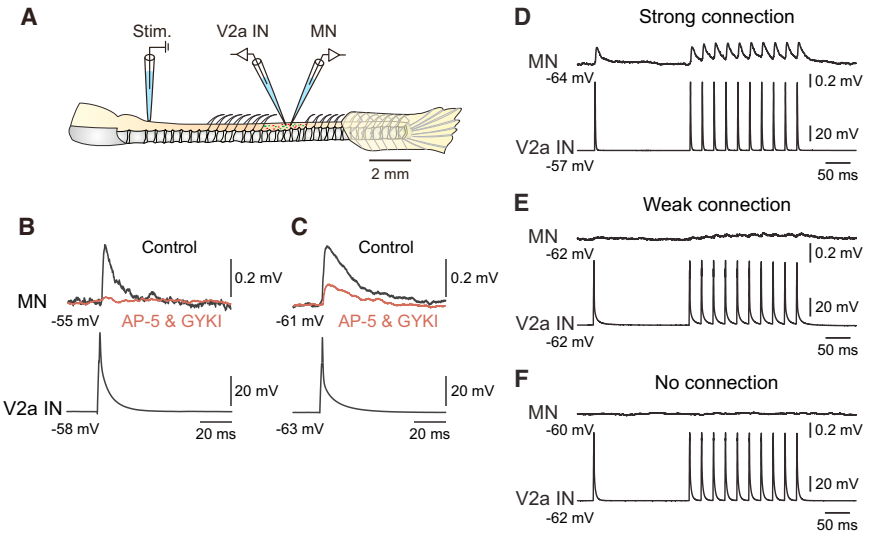

Figure 3. Nature of the Synaptic Interactions between V2a Interneurons and Motoneurons

(A) Experimental setup with the brainstem-spinal cord preparation. Dual whole-cell patch-clamp was made from identified V2a interneurons and motoneurons. Locomotion was induced by stimulation of descending axons from the brainstem using an extracellular stimulation electrode placed at the junction between the brainstem and spinal cord.

(B) In some pairs, the monosynaptic EPSPs induced in a motoneuron by a V2a interneuron was completely blocked by ionotropic glutamate receptor antagonists AP-5 (50 μM) and GYKI 52466 (30 μM).

(C) In other pairs (different pair than that in [B]), EPSPs were induced in motoneurons by stimulation of V2a interneurons that was not completely blocked by ionotropic glutamate receptor antagonists.

(D–F) The monosynaptic connections between V2a interneurons and motoneurons showed variable strengths. Strong connections were characterized by relatively large EPSPs (amplitude > 0.1 mV) that were elicited both by single and trains of action potentials in V2a interneurons (D). Weak connections were characterized by relatively small EPSPs (amplitude < 0.06 mV) elicited by single action potentials that summated during repetitive stimulation of the presynaptic V2a interneuron (E). No monosynaptic connections were detected, as no EPSPs were induced in motoneurons by either single or by trains of action potentials in presynaptic V2a interneurons (F).

that the locomotor network is organized into three discrete microcircuit modules with selective synaptic connections between V2a interneurons (rows in Figures 4A, 4C, and 4E) and motoneurons (columns in Figures 4A, 4C, and 4E) active at slow, intermediate, or fast locomotor frequencies. Indeed, slow V2a interneurons made strong and consistent monosynaptic connections with slow motoneurons (Figures 4A and 4B). In contrast, these slow V2a interneurons made only very weak and less frequent connections with intermediate motoneurons (Figure 4B) and made no connections with fast motoneurons (Figure 4B). Similarly, intermediate V2a interneurons made strong and reliable monosynaptic connections with intermediate motoneurons (Figures 4C and 4D). These intermediate V2a interneurons also made weak and sparse connections with both slow (Figure 4D) and fast motoneurons (Figure 4D). Finally, fast V2a interneurons made strong and consistent monosynaptic connections with fast motoneurons (Figures 4E and 4F). They made weak and less frequent connections only with intermediate motoneurons (Figure 4F) and not with slow motoneurons (Figure 4F).

The strength and distribution matrix of monosynaptic EPSPs (Figure 5A) clearly showed strong and reliable connections between V2a interneurons and motoneurons of functionally related modules and weak and sparse connections between interneurons and motoneurons of modules with adjacent recruitment frequencies (Figures 5B–5D). There was a clear segregation of the cumulative distribution of the EPSP amplitude from connections within the same module compared to connections between different modules (Figure 5B). These results demonstrate a functionally distinct organization of the locomotor network than previously recognized. This network is deconstructed into three discrete microcircuit modules with selective and strong synaptic connections between slow, intermediate, and fast V2a interneurons and motoneurons that mirror their order of recruitment during locomotion.

Organization of Synaptic Drive in the Different Microcircuit Modules

For the modular connectivity pattern to be functionally relevant, the excitation received during locomotion by the V2a interneurons and motoneurons of each microcircuit needs to be graded in a manner that enables their simultaneous recruitment. To examine this, we analyzed the locomotor-related excitatory drive to V2a interneurons and motoneurons at slow (<3 Hz) and fast (>8 Hz) locomotor frequencies. At slow frequencies, mostly neurons of the slow module are active while those of intermediate and fast modules are not (see Figure 4). The amplitude of the excitatory drive to V2a interneurons in relation to that of motoneurons of the same microcircuit module was correlated linearly (Figure 5E). The amplitude of the excitation of V2a interneurons and motoneurons of each microcircuit module was distributed in a continuum (Figure 5E). At these slow locomotor frequencies, the V2a interneurons and motoneurons of the slow module received largest excitatory input (red dots), while those of the fast module (blue dots) received the weakest excitation (Figure 5E). The excitatory drive received by V2a interneurons and motoneurons of the intermediate module (green dots) were distributed uniformly and bridged those of the slow and fast modules. At fast swimming frequencies, the amplitude of the excitation of V2a interneurons and motoneurons of the intermediate and fast modules increased significantly (Figure 5F). There was a large overlap of the amplitude of the excitation of V2a interneurons and motoneurons of slow, intermediate, and fast modules, reflecting their overlapping activation during fast swimming.

In contrast, there was no correlation between the amplitude of the excitatory drive of individual V2a interneurons in relation to

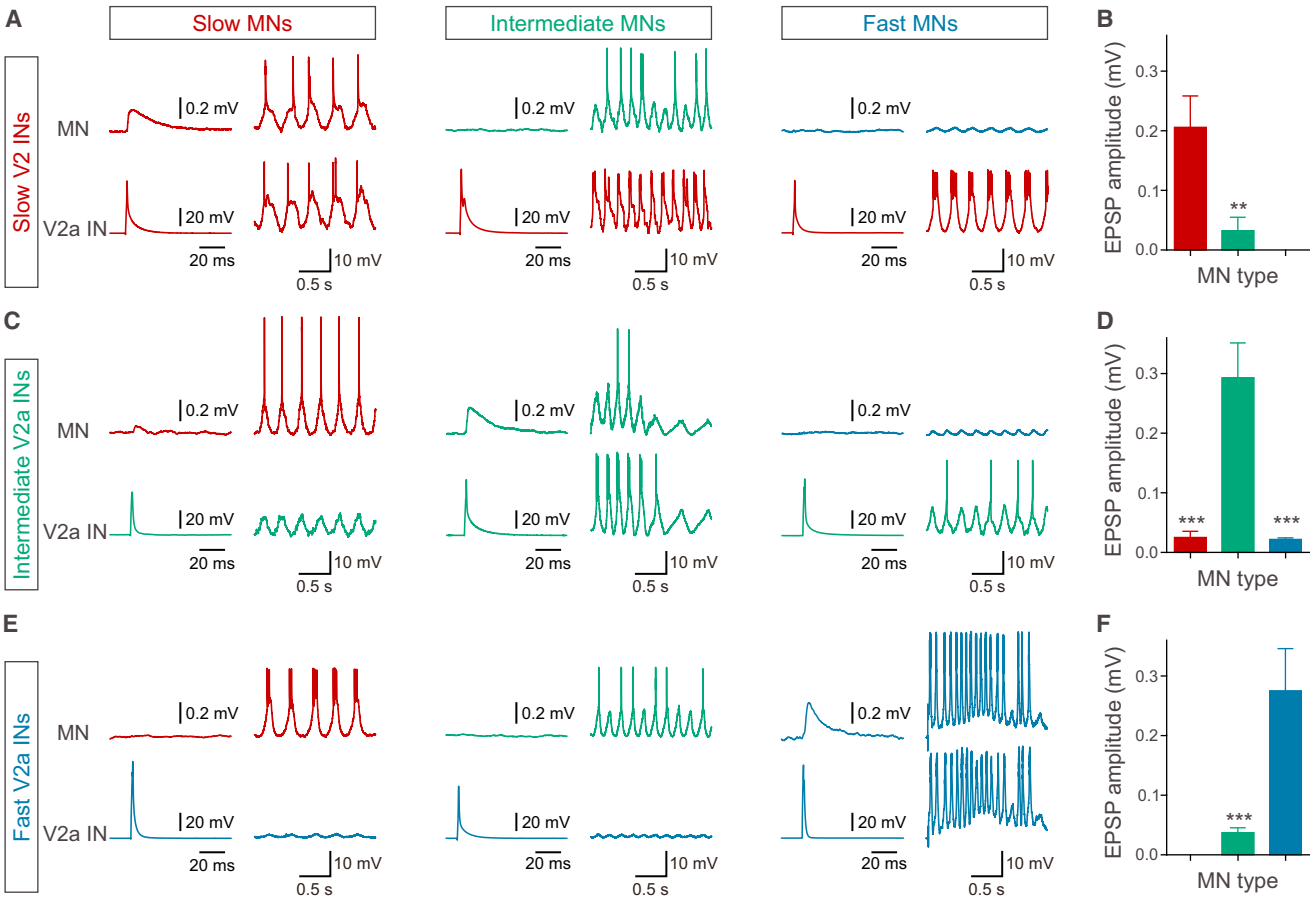

Figure 4. Modular Microcircuit Organization of the Locomotor Network

(A) Left panel: paired recordings showing the existence of a strong monosynaptic connection between a slow V2a interneuron (red) and a slow motoneuron (red) that were simultaneously recruited during swimming at slow speeds (3 Hz). Middle panel: paired recordings from a different slow V2a interneuron (red) and an intermediate motoneuron (green) without any detectable monosynaptic connections. These two neurons were recruited at intermediate swimming frequencies (7 Hz), as reveled by their simultaneous rhythmic firing. Right panel: paired recordings from a different slow V2a interneuron (red) and a fast motoneuron (blue) that were not monosynaptically connected. Only the slow V2a interneuron was recruited at slow/intermediate (6 Hz) swimming frequencies, while the motoneuron received subthreshold rhythmic synaptic inputs.

(B) Slow V2a interneurons induced reliable and strong monosynaptic EPSPs in slow motoneurons (0.22 ± 0.06 mV; mean ± SEM; n = 17 of 17 pairs), sparse and weak EPSPs in some intermediate motoneurons (0.03 ± 0.02 mV; mean ± SEM; n = 2 of 9 pairs), and no EPSPs in fast motoneurons (n = 0 of 13 pairs).

(C) Left panel: paired recordings showing the existence of a weak monosynaptic connection between an intermediate V2a interneuron (green) and a slow motoneuron (red) that were not simultaneously recruited during swimming at slow speeds (3 Hz). Middle panel: paired recordings a different intermediate V2a interneuron (green) and an intermediate motoneuron (green) showing a strong monosynaptic EPSP. These two neurons were recruited at intermediate swimming frequencies (7 Hz), as reveled by their simultaneous rhythmic firing. Right panel: paired recordings from a different intermediate V2a interneuron (green) and a fast motoneuron (blue) that were not monosynaptically connected. Only the intermediate V2a interneuron was recruited at intermediate swimming frequencies (6 Hz), while the fast motoneuron received subthreshold rhythmic synaptic inputs.

(D) Intermediate V2a interneurons induced reliable and strong monosynaptic EPSPs in intermediate motoneurons (0.29 ± 0.06 mV; mean ± SEM; n = 14 of 14 pairs) and sparse and weaker EPSPs in some slow (0.03 ± 0.01 mV; mean ± SEM; n = 3 of 9 pairs) as well as fast (0.02 ± 0.01 mV; mean ± SEM; n = 3 of 10 pairs) motoneurons.

(E) Left panel: paired recordings showing the lack of monosynaptic connections between a fast V2a interneuron (blue) and a slow motoneuron (red) that were not simultaneously recruited during swimming at slow speeds (2 Hz). Middle panel: paired recordings showing the lack of monosynaptic connections between a different fast V2a interneuron (blue) and an intermediate motoneuron (green). Only the intermediate motoneuron of this pair was recruited at intermediate swimming frequencies (6 Hz), while the fast V2a interneuron received subthreshold rhythmic synaptic inputs. Right panel: paired recording from a different fast V2a interneuron (blue) and a fast motoneuron (blue) that were strongly connected. These two neurons were recruited simultaneously at fast swimming frequencies (17 Hz).

(F) Fast V2a interneurons induced reliable and strong monosynaptic EPSPs in fast motoneurons (0.28 ± 0.07 mV; mean ± SEM; n = 18 of 18 pairs), sparse and weaker EPSPs in intermediate motoneurons (0.03 ± 0.01 mV; mean ± SEM; n = 6 of 13 pairs), and were never connected to slow motoneurons (n = 0 of 10 pairs).

motoneurons belonging to different microcircuit modules both at slow and fast swimming frequencies (Figures 5F and 5G). This organization of the excitatory drive to V2a interneurons and motoneurons within each microcircuit module allows for their gradual activation to increase the speed of locomotion. These results show that the excitation of the different microcircuit modules is

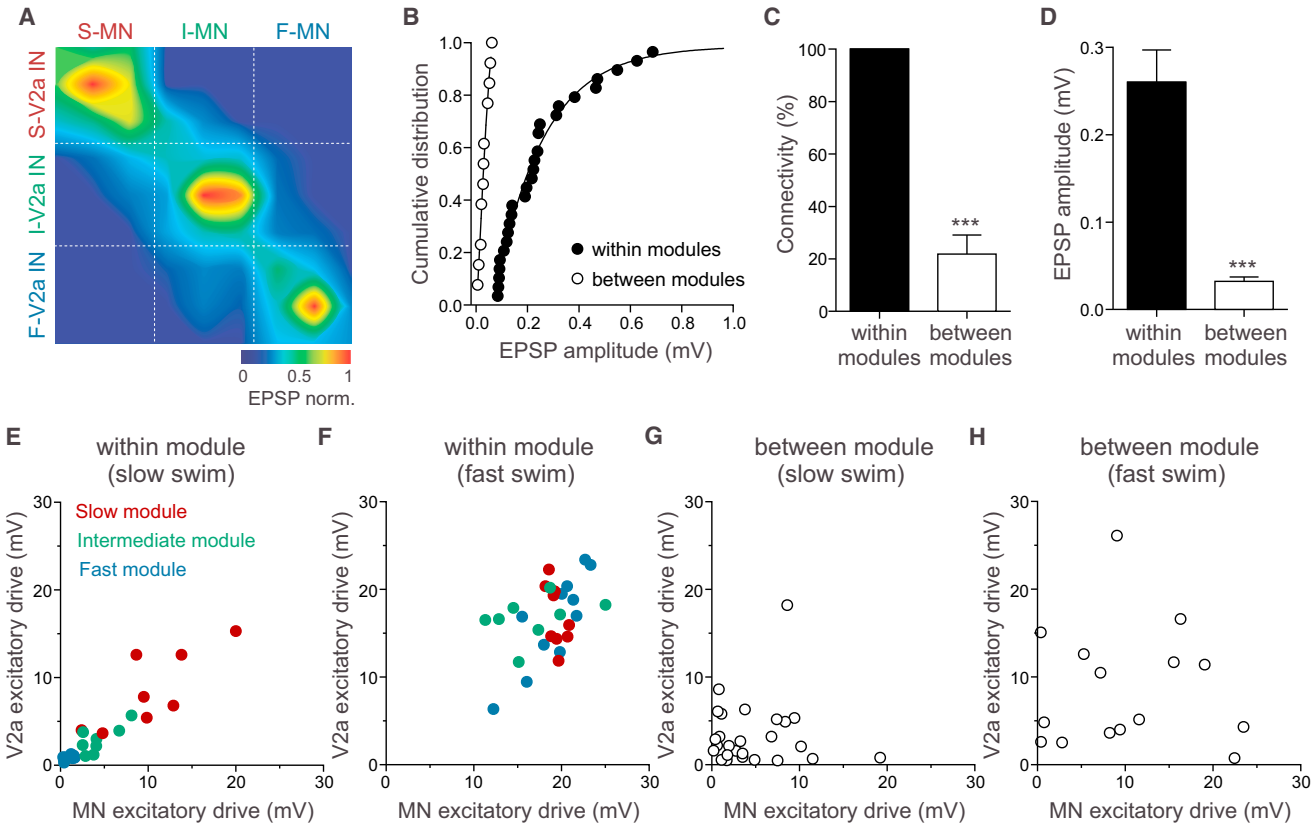

Figure 5. Scaling of the Excitation within the Different Microcircuit Modules

(A) Connectivity matrix showing the strength of the monosynaptic EPSPs between the different subclasses of V2a interneurons and motoneurons. The normalized EPSP amplitude from nine pairs of V2a interneurons and motoneurons of each combination were presented as a color gradient after interpolation.

(B) The EPSP amplitude between V2a interneurons and motoneurons of the same module was significantly larger than across modules.

(C) The existence of monosynaptic connections between V2a interneurons and motoneurons within each module was very reliable, while only a sparse pattern of connectivity was seen between V2a interneurons and motoneurons of different modules (mean ± SEM; $p < 0.001$).

(D) The EPSP amplitude was significantly (mean ± SEM; $p < 0.001$) larger in pairs of V2a interneurons and motoneurons of the same module than between modules.

(E) At slow locomotor frequencies (<3 Hz), there was a linear relationship ($R^2 = 0.8$) of the amplitude between the locomotor-related excitatory drive of the V2a interneurons in relation to that of the motoneurons of slow (red), intermediate (green), and fast (blue) module, respectively. The locomotor-related excitatory drive of V2a interneurons and motoneurons of the same module was organized in a continuum.

(F) At fast locomotor frequencies (>8 Hz), the amplitude of the locomotor-related excitatory drive of V2a interneurons and motoneurons of the different modules showed a large overlap. At fast swimming frequencies, there was an increase in the amplitude of the excitatory drive to V2a interneurons and motoneurons of intermediate (green) and fast (blue) modules compared to the amplitude seen at slow frequencies (see [E]).

(G and H) There is no relationship between the amplitude of the locomotor-related excitatory drive of V2a interneurons and motoneurons belonging to different modules both at slow and fast locomotor frequencies.

graded in a precise manner to ensure an incremental recruitment and hence a smooth transition of activity between motor units during acceleration and deceleration of locomotor speed.

Timing of the Activity of V2a Interneurons and Motoneurons during Locomotion

Is the activity of V2a interneurons and motoneurons temporally ordered to allow the excitation to be conveyed from the premotor circuits to motoneurons during locomotion? For V2a interneurons to drive the activity of the motoneurons, it is necessary that their first action potentials must precede those of motoneurons. The order of firing was determined by simultaneously recording from V2a interneurons and motoneurons. In each microcircuit module, the action potentials of V2a interneurons always occurred before those of motoneurons in each locomotor cycle (Figure 6A). There was a significant delay between the onset of firing of V2a interneurons and motoneurons of slow (9.0% ± 0.9% of cycle duration), intermediate (12.1% ± 0.9% of cycle duration), and fast (4.0% ± 0.3% of cycle duration) modules (Figure 6B). These results indicate that there is a tight temporal relationship between the activity of V2a interneurons and motoneurons within each microcircuit module to ensure that the interneurons are always active first and drive their respective pool of motoneurons.

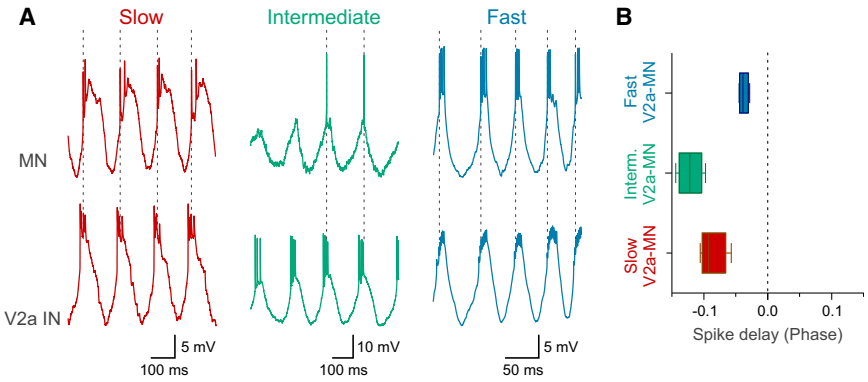

Figure 6. Temporal Relationship between the Activity of V2a Interneurons and Motoneurons

(A) The onset of action potential firing in slow, intermediate, and fast V2a interneurons always occurred prior to that of the corresponding motoneurons during locomotion.

(B) Graph showing the spike timing relationship between V2a interneurons and motoneurons. The delay was normalized to the cycle duration, and the dashed line represents the onset of spiking in motoneurons belonging to the corresponding module (slow, intermediate, or fast).

DISCUSSION

Modular Microcircuit Organization

Our results reveal an important principle of organization of the spinal locomotor circuits that accounts for the orderly activation of slow, intermediate, and fast motor units at different speeds of locomotion (Figure 7). In contrast to what has previously been assumed, we show that the locomotor network does not consist of a uniform unit, but can be deconstructed into three microcircuit modules. Each module includes a distinct subclass of excitatory V2a interneurons that make selective monosynaptic connections with slow, intermediate, or fast motoneurons. This modular organization of V2a interneurons-motoneurons combined with their overlapping activation during swimming ensures a smooth transition between locomotor speeds during acceleration or deceleration by sequentially engaging or disengaging the successive microcircuits.

The prevailing concept is that the recruitment of motor units follows the "size principle," which assumes that all motoneurons from slow to fast receive homogenous and uniformly distributed excitatory inputs from a common premotor source and that their order of activation is dictated by their input resistance. Our results invalidate this crucial assumption of the "size principle." We show that the locomotor network does not convey equal and uniformly distributed excitatory drive to slow, intermediate, and fast motoneurons. Rather, the excitatory drive to motoneurons is channeled in a specific and selective pattern according to a precise connectivity map within the locomotor circuits. Thus, slow, intermediate, and fast microcircuit modules of V2a interneurons and motoneurons emerge that reflect the properties of the motor units and their orderly sequence of recruitment during movements with increased speed and force.

Functional Role and Diversity of V2a Interneurons

Our analysis shows that the V2a interneurons form a functionally heterogeneous class that can be segregated into three distinct subclasses. The V2a interneurons of each subclass are activated at a specific frequency threshold during locomotion and are selectively connected to slow, intermediate, or fast motoneurons. In addition, their spike threshold and excitatory synaptic drives (Ausborn et al., 2012) are tuned in a manner that correlates with their orderly sequence of activation during swimming with increased speed.

Several lines of evidence indicate that V2a interneurons are the major source of intrinsic excitation underlying the locomotor rhythm generation in zebrafish. We previously showed the following: (1) V2a interneurons contribute to the excitatory drive necessary for the normal expression of locomotion because their acute ablation decreases the swimming burst frequency (Eklöf-Ljunggren et al., 2012), (2) direct activation of V2a interneurons alone using optogenetic tools is sufficient to generate coordinated locomotor activity (Eklöf Ljunggren et al., 2014), and (3) selective optogenetic stimulation of V2a interneurons produces synaptic excitation in other interneurons of the same class, suggesting that they form an interconnected network (Eklöf Ljunggren et al., 2014). Thus, the V2a interneurons contribute critically to the generation of the locomotor rhythm and convey the rhythmic drive to the different motoneurons. The incremental recruitment of slow, intermediate, and fast V2a interneuron subclasses by descending inputs from the brainstem command centers could provide increasing excitatory drive to regulate the swimming frequency. The organization of the descending excitatory drive to the different V2a subclasses remains to be elucidated.

The existence of monosynaptic connections between excitatory interneurons and motoneurons has been previously demonstrated electrophysiologically only in lamprey and *Xenopus* tadpoles (Buchanan and Grillner, 1987; Buchanan et al., 1989; Dale and Roberts, 1985; Grillner, 2003; Roberts et al., 2010, 2012). In zebrafish embryos and larvae, V2a interneurons have been shown to excite primary motoneurons (Kimura et al., 2006). Recently, in mammals the existence of monosynaptic connections between excitatory interneurons and motoneurons has been revealed anatomically by using monosynaptic rabies virus (Stepien et al., 2010; Tripodi et al., 2011; Zampieri et al., 2014). However, in none of these previous studies has it been possible to segregate the excitatory interneurons into different functional classes and functionally relate them to their connectivity scheme with the different types of motoneurons. The adult zebrafish allows for such types of analysis because different V2a interneurons and motoneurons are readily accessible, and their activity pattern can be examined during swimming at different speeds.

In newborn rodents, genetic ablation of V2a interneurons early during development disrupted the initiation of locomotor-like activity by descending or sensory inputs but did not affect

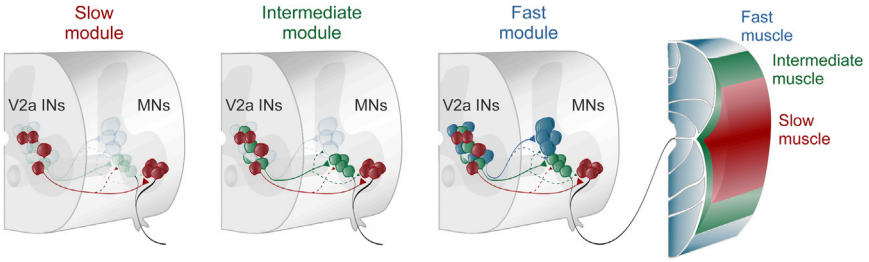

Figure 7. Modular Microcircuit Organization of the Spinal Locomotor Network
The modular microcircuit organization endows the spinal cord with an intrinsic gearshift that allows an increase in the locomotor speed by incrementally recruiting slow, intermediate, and fast V2a interneuron-motoneuron modules. This organization enables selective recruitment of subsets of microcircuits to produce locomotion with the desired speed.

the frequency of drug-induced rhythm (Crone et al., 2008, 2009). Rather, there was a significant change in the reciprocal coordination that was more apparent at a relatively higher frequency (Crone et al., 2008, 2009). In mammals, there is thus far no electrophysiological evidence for the existence of chemical synaptic connections within the V2a interneuron class or with motoneurons (Dougherty and Kiehn, 2010). However, there are some discrepancies with regard to the existence of electrical coupling between V2a interneurons in newborn rodents in two different studies (Dougherty and Kiehn, 2010; Zhong et al., 2010).

Microcircuit Modules and Locomotor Speed Control

The segregation of V2a interneurons into three distinct classes relates to their connectivity to slow, intermediate, and fast motoneuron pools in the adult stage, when all muscle types are fully developed (Devoto et al., 1996; van Raamsdonk et al., 1982). At larval stages, the slow and intermediate muscles are not yet differentiated, and swimming relies almost entirely on fast motoneurons (Drapeau et al., 2002; Masino and Fetcho, 2005; McLean et al., 2007; van Raamsdonk et al., 1982). In embryonic and larval zebrafish, V2a interneurons are active during strong or weak movements according to their sequence of development (Kimura et al., 2006; McLean and Fetcho, 2009).

The three microcircuit modules revealed in adult zebrafish could be the consequence of a specific rewiring of existing V2a interneurons and motoneurons that adapts to the differentiation of intermediate and slow muscles. Alternatively, it is possible that new microcircuit layers are differentiated later during development to match that of intermediate and slow muscles. While in this study the multiple microcircuits organization reveals how the excitatory drive from the locomotor network is selectively conveyed from a specific V2a interneuron class to a defined pool of motoneurons, the left-right coordination of the activity within each microcircuit module relies on reciprocal inhibition from commissural interneurons. These interneurons are either excitatory or inhibitory (Satou et al., 2012). It is possible that they could also be segregated into different subclasses that can serve to coordinate the activity within slow, intermediate, and fast microcircuit module, respectively.

General Implications

A hitherto unappreciated principle of organization of the spinal locomotor circuits thus emerges from our study in the adult zebrafish. This selective and modular design enables the increase of locomotor speed by sequentially engaging successive microcircuit layers from slow to intermediate and fast. In mammals, the muscles and the corresponding motor pools mostly contain a mix of slow, intermediate, and fast muscle fibers and motoneurons, respectively (Arber, 2012; Burke, 2011; Dasen and Jessell, 2009; Henneman and Mendell, 1981). An implication of our results is that the slow, intermediate, and fast motoneurons within each mammalian motor pool may also form discrete microcircuits, each with a distinct class of excitatory premotor interneurons. In mammals, such a modular microcircuit organization would optimize synergies by engaging and selectively coordinating slow, intermediate, and fast motor units across synergistic motor pools.

Our findings show that the orderly activation of motor units is not exclusively assigned to motoneurons as has been assumed by the "size principle." Rather, it emerges from the precise and selective principle of connectivity between excitatory interneurons and motoneurons that ultimately reflects the muscle fiber properties (Figure 7). The coordination of the activity across modules also has implications for the synaptic interactions between the excitatory interneurons, although the precise pattern of such interactions remains to be elucidated. Nevertheless, the present study has provided new insights into how excitation is channeled to different motoneuron pools and how it defines their recruitment order. Thus, the modular microcircuit organization uncovered here endows the spinal locomotor circuits with an intrinsic gearshift mechanism to increase the speed by incrementally engaging different motor units.

EXPERIMENTAL PROCEDURES

Zebrafish (*Danio rerio*) were raised and kept in a core facility at the Karolinska Institute according to established procedures. To enable selective targeting of V2a interneurons we used a zebrafish line (Chx10:GFP) in which the expression of GFP was driven in V2a interneurons by the promoter of the transcription factor Alx (homolog of Chx10) (Ausborn et al., 2012; Kimura et al., 2006). All experimental protocols were approved by the local Animal Research Ethical Committee, Stockholm, and were performed in accordance with EU guidelines.

Retrograde labeling of motoneurons was performed using Rhodamine-dextran (3,000 MW, Molecular Probes) in 8- to 10-week-old zebrafish (Ampatzis et al., 2013; Gabriel et al., 2008, 2011). The animals were anaesthetized in 0.03% tricaine methane sulfonate (MS-222, Sigma-Aldrich), and the fluorescent dye was injected into separate or all muscle types using dye-soaked pins in order to sever the motor axons and allow for successful uptake of the dye. The injected animals were allowed to recover overnight to help the retrograde transport of the tracer. To reveal the position of all motoneurons and V2a interneurons within the spinal segment, animals were deeply anesthetized with 0.1% MS-222 and intracardially perfused with 4% paraformaldehyde (PFA) in phosphate buffer (PB) (0.1M; pH = 7.4). The spinal cord was dissected out and post-fixed in 4% PFA solution overnight at 4°C. The tissue was then processed for single immunohistochemical labeling against GFP. The spinal cords were washed three times for 5 min in PBS (0.01M PBS;

pH = 7.4). Nonspecific protein binding sites were blocked with 0.15% normal horse serum with 5% BSA and 1% Triton X-100 in PBS for 30 min at room temperature. Spinal cords were then incubated with rabbit anti-GFP in 1% Triton X-100 in PBS at 4°C for 72 hr. After thorough buffer rinses the tissue was incubated with anti-rabbit Alexa Fluor 488 antibody overnight at 4°C and subsequently rinsed in PBS and coverslipped with antifade fluorescent mounting medium (Vectashield Hard Set, Vector Labs). Whole-mount imaging of the spinal cords was carried out in a laser scanning confocal microscope (LSM 510 Meta, Zeiss). The relative position of the somata of the motoneurons and the V2a interneurons was calculated using the lateral, dorsal, and ventral edges of the spinal cord as well as the central canal as landmarks.

Zebrafish were cold anesthetized in a slush of frozen extracellular solution containing MS-222 and were eviscerated. The brainstem-spinal cord was dissected out and transferred to a recording chamber that was continuously perfused with an extracellular solution containing the following (in mM): 134 NaCl, 2.9 KCl, 2.1 $CaCl_2$, 1.2 $MgCl_2$, 10 HEPES, and 10 glucose with pH 7.8 adjusted with NaOH and an osmolarity of 290 mOsm. D-tubocurarine (10 μM, Sigma-Aldrich) was added to the extracellular solution to block neuromuscular junctions and to eliminate muscle contractions for the whole duration of the experiment. All experiments were performed at an ambient temperature of 20°C–22°C.

Fictive locomotion was induced by extracellular stimulation using a glass pipette that was placed at the junction between the brainstem and spinal cord (Ampatzis et al., 2013; Ausborn et al., 2012; Kyriakatos et al., 2011). Whole-cell patch-clamp recordings were performed from identified secondary motoneurons prelabeled with a retrograde tracer and from GFP-positive V2a interneurons. The intracellular solution contained the following (in mM): 120 K-gluconate, 5 KCl, 10 HEPES, 4 Mg_2ATP, 0.3 Na_4GTP, and 10 Na-phosphocreatine with pH 7.4 adjusted with KOH and an osmolarity of 275 mOsm. Dextran-labeled secondary motoneurons and GFP-labeled V2a interneurons were visualized using a fluorescence microscope (Axioskop FS Plus; Zeiss) equipped with IR-differential interference contrast optics and a CCD camera with frame grabber (Hamamatsu) and were then targeted specifically. Two patch-clamp electrodes were advanced, from opposite directions, into the spinal cord through the meninges using motorized micromanipulators while applying constant positive pressure. Intracellular signals were amplified with a MultiClamp 700B intracellular amplifier (Molecular Devices) and low-pass filtered at 10 kHz. In current-clamp recordings, no bias current was injected. Only motoneurons and V2a interneurons that had stable membrane potentials at or below −48 mV, fired action potentials to suprathreshold depolarizations, and showed minimal changes in series resistance (<5%) were included in this study. Single and multiple short-duration current pulses were used to stimulate presynaptic V2a interneurons and record EPSPs in secondary motoneurons. Electrical coupling was tested by injecting long depolarizing and hyperpolarizing current pulses in V2a interneurons and motoneurons. The excitatory nature of the chemical synaptic transmission was determined by using ionotropic glutamate receptors antagonists (AP-5 and GYKI 52466).

The distribution of V2a interneurons was analyzed in a specific segment located rostral to the dorsal fin that corresponds to the region where intracellular recordings were made. The lateral edge of the Mauthner axon was set as the zero point of the mediolateral axis. The dorsoventral position was set relative to the Mauthner axon and the dorsal edge of the spinal cord. The analysis of the electrophysiological data was performed using Spike2 (Cambridge Electronic Design) or Clampfit (Molecular Devices) software. The minimum recruitment frequency of motoneurons and V2a interneurons was defined as the slowest burst frequency of a swimming episode at which the neurons discharged action potentials at least during two consecutive cycles. The action potential voltage threshold of V2a interneurons was determined from the measured membrane potential at which the dV/dt exceeded 10 $V \cdot s^{-1}$. The dual recording traces illustrated represent averages of 60–100 consecutive sweeps. The EPSP amplitude was calculated as the difference between baseline and peak. The excitatory drive to secondary motoneurons and V2a interneurons was calculated at the difference between the peak depolarization during locomotion and the resting membrane potential measured before the onset of swimming and averaged over five to ten locomotor cycles. The phase delay of the spike appearance between the motoneurons, and the V2a interneurons was calculated by measuring the time between the first spike of these neurons in each locomotor cycle for five to ten continuous cycles and normalized to the cycle period. The significance of differences between the means in experimental groups and conditions was analyzed using the Student's two-tailed t test using Prism 4.0 (GraphPad Software Inc.) Differences were considered to be significant if $p < 0.05$. All data presented here are given as mean ± SEM.

AUTHOR CONTRIBUTIONS

K.A., J.S., and A.E.M. conceived the study and designed the experiments. K.A., J.S. and J.A. performed the experiments. All the authors contributed to the analysis of the data and preparation of the manuscript.

ACKNOWLEDGMENTS

We thank R. Björnfors, R. Calabrese, S. Grillner, and O. Kiehn for comments and critical discussion of this manuscript and A. A. Kardamakis for help and advice with analysis. We are grateful to S. Higashijima and J. Fetcho for providing the transgenic line used in this study. This was work was supported by a grant from the Swedish Research Council, StratNeuro, and the Karolinska Institute.

Accepted: July 8, 2014
Published: August 7, 2014

REFERENCES

Ampatzis, K., Song, J., Ausborn, J., and El Manira, A. (2013). Pattern of innervation and recruitment of different classes of motoneurons in adult zebrafish. J. Neurosci. *33*, 10875–10886.

Arber, S. (2012). Motor circuits in action: specification, connectivity, and function. Neuron *74*, 975–989.

Ausborn, J., Mahmood, R., and El Manira, A. (2012). Decoding the rules of recruitment of excitatory interneurons in the adult zebrafish locomotor network. Proc. Natl. Acad. Sci. USA *109*, E3631–E3639.

Bernhardt, R.R., Chitnis, A.B., Lindamer, L., and Kuwada, J.Y. (1990). Identification of spinal neurons in the embryonic and larval zebrafish. J. Comp. Neurol. *302*, 603–616.

Buchanan, J.T., and Grillner, S. (1987). Newly identified 'glutamate interneurons' and their role in locomotion in the lamprey spinal cord. Science *236*, 312–314.

Buchanan, J.T., Grillner, S., Cullheim, S., and Risling, M. (1989). Identification of excitatory interneurons contributing to generation of locomotion in lamprey: structure, pharmacology, and function. J. Neurophysiol. *62*, 59–69.

Burke, R.E. (2011). Motor units: anatomy, physiology, and functional organization. Comprehensive Physiology, 345–422, http://dx.doi.org/10.1002/cphy.cp010210.

Büschges, A., Scholz, H., and El Manira, A. (2011). New moves in motor control. Curr. Biol. *21*, R513–R524.

Cope, T.C., and Pinter, M.J. (1995). The Size Principle: Still Working After All These Years. News Physiol. Sci. *10*, 280–286.

Crone, S.A., Quinlan, K.A., Zagoraiou, L., Droho, S., Restrepo, C.E., Lundfald, L., Endo, T., Setlak, J., Jessell, T.M., Kiehn, O., and Sharma, K. (2008). Genetic ablation of V2a ipsilateral interneurons disrupts left-right locomotor coordination in mammalian spinal cord. Neuron *60*, 70–83.

Crone, S.A., Zhong, G., Harris-Warrick, R., and Sharma, K. (2009). In mice lacking V2a interneurons, gait depends on speed of locomotion. J. Neurosci. *29*, 7098–7109.

Dale, N., and Roberts, A. (1985). Dual-component amino-acid-mediated synaptic potentials: excitatory drive for swimming in Xenopus embryos. J. Physiol. *363*, 35–59.

Dasen, J.S., and Jessell, T.M. (2009). Hox networks and the origins of motor neuron diversity. Curr. Top. Dev. Biol. *88*, 169–200.

Devoto, S.H., Melançon, E., Eisen, J.S., and Westerfield, M. (1996). Identification of separate slow and fast muscle precursor cells in vivo, prior to somite formation. Development *122*, 3371–3380.

Dougherty, K.J., and Kiehn, O. (2010). Functional organization of V2a-related locomotor circuits in the rodent spinal cord. Ann. N Y Acad. Sci. *1198*, 85–93.

Drapeau, P., Saint-Amant, L., Buss, R.R., Chong, M., McDearmid, J.R., and Brustein, E. (2002). Development of the locomotor network in zebrafish. Prog. Neurobiol. *68*, 85–111.

Eklöf-Ljunggren, E., Haupt, S., Ausborn, J., Dehnisch, I., Uhlén, P., Higashijima, S.I., and El Manira, A. (2012). Origin of excitation underlying locomotion in the spinal circuit of zebrafish. Proc. Natl. Acad. Sci. USA *109*, 5511–5516.

Gabriel, J.P., Mahmood, R., Walter, A.M., Kyriakatos, A., Hauptmann, G., Calabrese, R.L., and El Manira, A. (2008). Locomotor pattern in the adult zebrafish spinal cord in vitro. J. Neurophysiol. *99*, 37–48.

Gabriel, J.P., Ausborn, J., Ampatzis, K., Mahmood, R., Eklöf-Ljunggren, E., and El Manira, A. (2011). Principles governing recruitment of motoneurons during swimming in zebrafish. Nat. Neurosci. *14*, 93–99.

Goulding, M. (2009). Circuits controlling vertebrate locomotion: moving in a new direction. Nat. Rev. Neurosci. *10*, 507–518.

Grillner, S. (2003). The motor infrastructure: from ion channels to neuronal networks. Nat. Rev. Neurosci. *4*, 573–586.

Grillner, S., and Jessell, T.M. (2009). Measured motion: searching for simplicity in spinal locomotor networks. Curr. Opin. Neurobiol. *19*, 572–586.

Gustafsson, B., and Pinter, M.J. (1984). An investigation of threshold properties among cat spinal alpha-motoneurones. J. Physiol. *357*, 453–483.

Hale, M.E., Ritter, D.A., and Fetcho, J.R. (2001). A confocal study of spinal interneurons in living larval zebrafish. J. Comp. Neurol. *437*, 1–16.

Henneman, E. (1957). Relation between size of neurons and their susceptibility to discharge. Science *126*, 1345–1347.

Henneman, E., and Mendell, L.M. (1981). Functional organization of motoneuron pool and its inputs. In Handbook of Physiology, *Volume 2*, V.E. Brooks, ed. (Bethesda, MD: American Physiological Society), pp. 423–507.

Hoffer, J.A., Sugano, N., Loeb, G.E., Marks, W.B., O'Donovan, M.J., and Pratt, C.A. (1987). Cat hindlimb motoneurons during locomotion. II. Normal activity patterns. J. Neurophysiol. *57*, 530–553.

Kiehn, O. (2006). Locomotor circuits in the mammalian spinal cord. Ann. Rev. Neurosci. *29*, 279–306.

Kimura, Y., Okamura, Y., and Higashijima, S. (2006). alx, a zebrafish homolog of Chx10, marks ipsilateral descending excitatory interneurons that participate in the regulation of spinal locomotor circuits. J. Neurosci. *26*, 5684–5697.

Kimura, Y., Satou, C., Fujioka, S., Shoji, W., Umeda, K., Ishizuka, T., Yawo, H., and Higashijima, S. (2013). Hindbrain V2a neurons in the excitation of spinal locomotor circuits during zebrafish swimming. Curr. Biol. *23*, 843–849.

Kyriakatos, A., Mahmood, R., Ausborn, J., Porres, C.P., Büschges, A., and El Manira, A. (2011). Initiation of locomotion in adult zebrafish. J. Neurosci. *31*, 8422–8431.

Lewis, K.E., and Eisen, J.S. (2003). From cells to circuits: development of the zebrafish spinal cord. Prog. Neurobiol. *69*, 419–449.

Liddell, E.G.T., and Sherrington, C.S. (1925). Recruitment and some other factors of reflex inhibition. Proc. R. Soc. Lond., B *97*, 488–518.

Ljunggren, E.E., Haupt, S., Ausborn, J., Ampatzis, K., and El Manira, A. (2014). Optogenetic activation of excitatory premotor interneurons is sufficient to generate coordinated locomotor activity in larval zebrafish. J. Neurosci. *34*, 134–139.

Masino, M.A., and Fetcho, J.R. (2005). Fictive swimming motor patterns in wild type and mutant larval zebrafish. J. Neurophysiol. *93*, 3177–3188.

McLean, D.L., and Fetcho, J.R. (2009). Spinal interneurons differentiate sequentially from those driving the fastest swimming movements in larval zebrafish to those driving the slowest ones. J. Neurosci. *29*, 13566–13577.

McLean, D.L., Fan, J., Higashijima, S., Hale, M.E., and Fetcho, J.R. (2007). A topographic map of recruitment in spinal cord. Nature *446*, 71–75.

McLean, D.L., Masino, M.A., Koh, I.Y., Lindquist, W.B., and Fetcho, J.R. (2008). Continuous shifts in the active set of spinal interneurons during changes in locomotor speed. Nat. Neurosci. *11*, 1419–1429.

Roberts, A., Li, W.C., and Soffe, S.R. (2010). How neurons generate behavior in a hatchling amphibian tadpole: an outline. Front. Behav. Neurosci. *4*, 16.

Roberts, A., Li, W.C., and Soffe, S.R. (2012). A functional scaffold of CNS neurons for the vertebrates: the developing Xenopus laevis spinal cord. Dev. Neurobiol. *72*, 575–584.

Romanes, G.J. (1964). The Motor Pools of the Spinal Cord. Prog. Brain Res. *11*, 93–119.

Satou, C., Kimura, Y., and Higashijima, S. (2012). Generation of multiple classes of V0 neurons in zebrafish spinal cord: progenitor heterogeneity and temporal control of neuronal diversity. J. Neurosci. *32*, 1771–1783.

Stepien, A.E., Tripodi, M., and Arber, S. (2010). Monosynaptic rabies virus reveals premotor network organization and synaptic specificity of cholinergic partition cells. Neuron *68*, 456–472.

Tripodi, M., Stepien, A.E., and Arber, S. (2011). Motor antagonism exposed by spatial segregation and timing of neurogenesis. Nature *479*, 61–66.

van Raamsdonk, W., van't Veer, L., Veeken, K., Heyting, C., and Pool, C.W. (1982). Differentiation of muscle fiber types in the teleost Brachydanio rerio, the zebrafish. Posthatching development. Anat. Embryol. (Berl.) *164*, 51–62.

Zampieri, N., Jessell, T.M., and Murray, A.J. (2014). Mapping sensory circuits by anterograde transsynaptic transfer of recombinant rabies virus. Neuron *81*, 766–778.

Zhang, H.Y., Issberner, J., and Sillar, K.T. (2011). Development of a spinal locomotor rheostat. Proc. Natl. Acad. Sci. USA *108*, 11674–11679.

Zhong, G., Droho, S., Crone, S.A., Dietz, S., Kwan, A.C., Webb, W.W., Sharma, K., and Harris-Warrick, R.M. (2010). Electrophysiological characterization of V2a interneurons and their locomotor-related activity in the neonatal mouse spinal cord. J. Neurosci. *30*, 170–182.